AGU PUBLICATIONS

JGR

Journal of Geophysical Research: Biogeosciences

RESEARCH ARTICLE

10.1002/2013JG002587

Key Points:
- Marine CDOM accumulated during the experiment as a result of bacterial activity
- No change in CDOM accumulation in response to increased pCO2
- There were found prominent mycosporine-like amino acids (MAA) absorption peaks

Correspondence to:
A. K. Pavlov,
pavlov.alexey.k@gmail.com

Citation:
Pavlov, A. K., A. Silyakova, M. A. Granskog, R. G. J. Bellerby, A. Engel, K. G. Schulz, and C. P. D. Brussaard (2014), Marine CDOM accumulation during a coastal Arctic mesocosm experiment: No response to elevated pCO_2 levels, *J. Geophys. Res. Biogeosci.*, *119*, 1216–1230, doi:10.1002/2013JG002587.

Received 5 DEC 2013
Accepted 16 MAY 2014
Accepted article online 22 MAY 2014
Published online 20 JUN 2014

Marine CDOM accumulation during a coastal Arctic mesocosm experiment: No response to elevated pCO_2 levels

Alexey K. Pavlov[1,2], Anna Silyakova[3,4,5], Mats A. Granskog[1], Richard G.J. Bellerby[6,4,5], Anja Engel[7], Kai G. Schulz[7,8], and Corina P.D. Brussaard[9]

[1]Norwegian Polar Institute, Fram Centre, Tromsø, Norway, [2]Arctic and Antarctic Research Institute, St. Petersburg, Russia, [3]Centre for Arctic Gas hydrate, Environment and Climate, Department of Geology, UiT The Arctic University of Norway, Tromsø, Norway, [4]Uni Bjerknes Centre, Bergen, Norway, [5]Bjerknes Center for Climate Research, Bergen, Norway, [6]Norwegian Institute for Water Research, Bergen, Norway, [7]GEOMAR, Helmholtz Centre for Ocean Research Kiel, Kiel, Germany, [8]Centre for Coastal Biogeochemistry, School of Environmental Science and Management, Southern Cross University, Lismore, Australia, [9]Royal Netherlands Institute for Sea Research (NIOZ), Texel, Netherlands

Abstract A large-scale multidisciplinary mesocosm experiment in an Arctic fjord (Kongsfjorden, Svalbard; 78°56.2′N) was used to study Arctic marine food webs and biogeochemical elements cycling at natural and elevated future carbon dioxide (CO_2) levels. At the start of the experiment, marine-derived chromophoric dissolved organic matter (CDOM) dominated the CDOM pool. Thus, this experiment constituted a convenient case to study production of autochthonous CDOM, which is typically masked by high levels of CDOM of terrestrial origin in the Arctic Ocean proper. CDOM accumulated during the experiment in line with an increase in bacterial abundance; however, no response was observed to increased pCO_2 levels. Changes in CDOM absorption spectral slopes indicate that bacteria were most likely responsible for the observed CDOM dynamics. Distinct absorption peaks (at ~ 330 and ~ 360 nm) were likely associated with mycosporine-like amino acids (MAAs). Due to the experimental setup, MAAs were produced in absence of ultraviolet exposure providing evidence for MAAs to be considered as multipurpose metabolites rather than simple photoprotective compounds. We showed that a small increase in CDOM during the experiment made it a major contributor to total absorption in a range of photosynthetically active radiation (PAR, 400–700 nm) and, therefore, is important for spectral light availability and may be important for photosynthesis and phytoplankton groups composition in a rapidly changing Arctic marine ecosystem.

1. Introduction

The Arctic has undergone significant transformations over the past decades [*Arctic Monitoring and Assessment Programme* (*AMAP*), 2011; *Intergovernmental Panel on Climate Change*, 2013]. There has been a dramatic decrease in the extent, thickness, and volume of Arctic sea ice [*Stroeve et al*., 2012; *Laxon et al*., 2013], warming of the Atlantic Water inflow to the Arctic Ocean [*Polyakov et al*., 2005, 2011; *Walczowski and Piechura*, 2007], increasing freshwater discharge [*Peterson et al*., 2002] which in turn can increase the supply of terrigenous organic material [*Stedmon et al*., 2011], as will increased rates of coastal permafrost erosion and thawing [*Arctic Climate Impact Assessment*, 2005; *Vonk et al*., 2012]. Additionally, changes in biogeochemical element cycling including rapid increase in Arctic Ocean acidity [*AMAP*, 2013], occurrence of stratospheric ozone depletions over the Arctic [*Manney et al*., 2011], and other ongoing changes may have far reaching consequences for the fragile Arctic marine ecosystem [*Post et al*., 2013].

Light availability is of paramount importance for photosynthesis and productivity of organic matter in the upper layer of the Arctic Ocean and is the primary driver in summer and a limiting factor in winter [*Arrigo et al*., 2008; *Popova et al*., 2012]. With diminishing Arctic sea ice cover, a thorough description of processes and factors controlling the underwater light regime is crucial to better understand the current state and better project the future of the Arctic marine biological productivity [*Popova et al*., 2012; *Bélanger et al*., 2013].

In this context, a significant role of chromophoric dissolved organic matter (CDOM) in the Arctic Ocean has been recently recognized [*Granskog et al*., 2007; *Hill*, 2008]. CDOM is an optically active fraction of the dissolved organic matter (DOM) that absorbs light in the ultraviolet (UV) and visible bands [*Bricaud et al*., 1981]

©2014. American Geophysical Union. All Rights Reserved.

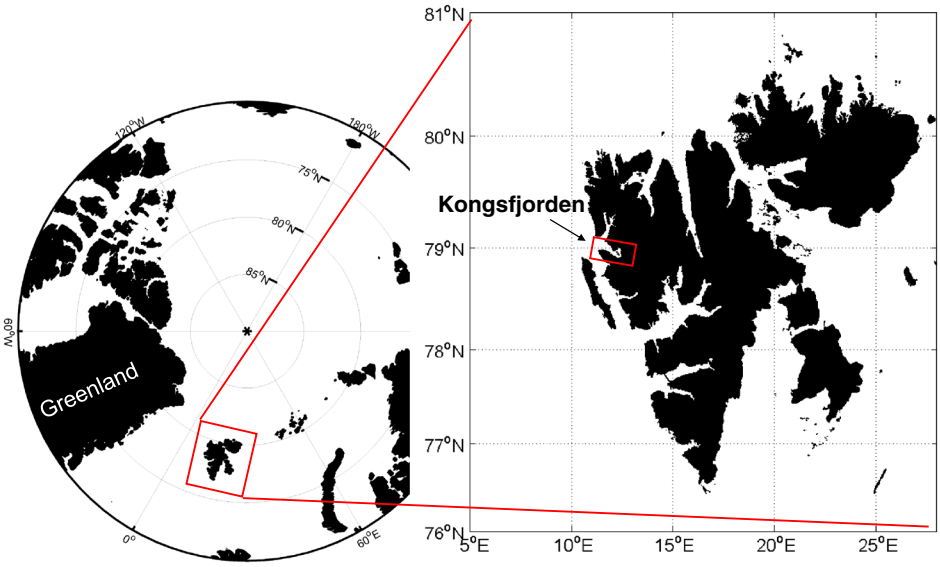

Figure 1. Map of the Arctic Ocean with the Svalbard archipelago highlighted in red and enlarged map of the latter with a red square indicating the location of Kongsfjorden.

and can originate from both terrestrial and marine sources [*Blough and Del Vecchio*, 2002]. The Arctic Ocean receives substantial riverine input of terrestrial organic matter including CDOM [e.g., *Dittmar and Kattner*, 2003; *Stedmon et al*., 2011]. The presence of CDOM profoundly affects the physics, biogeochemistry, and biology in the upper layer of the Arctic Ocean through radiative heating [*Pegau*, 2002; *Granskog et al*., 2007; *Hill*, 2008], availability of photosynthetically active radiation (PAR) for photosynthesis [*Granskog et al*., 2007], photoprotection of marine organisms from harmful UV light [*Gibson et al*., 2000], and photochemical transformation of organic matter [*Osburn et al*., 2009]. Practically, due to its effect on remotely sensed ocean color, CDOM must be properly taken into consideration when primary productivity is assessed in the Arctic Ocean [*Matsuoka et al*., 2007; *Popova et al*., 2012; *Bélanger et al*., 2013].

Despite its apparent importance, there are still many uncertainties and gaps in our understanding of CDOM dynamics and behavior in the Arctic Ocean. To date, the majority of CDOM studies in the Arctic Ocean focused on CDOM of terrestrial origin [*Dittmar and Kattner*, 2003; *Spencer et al*., 2009; *Stedmon et al*., 2011; *Granskog et al*., 2012], which is ubiquitous in the Arctic and is often masking marine autochthonous CDOM. Therefore, even less is known about production and properties of the apparently more labile marine CDOM in the Arctic Ocean.

Here we investigate production and properties of marine CDOM under a range of seawater CO_2 concentrations during a high-latitude mesocosm experiment on ocean acidification in the Arctic (EPOCA campaign) [see *Riebesell et al*., 2013a].

2. Material and Methods

2.1. Mesocosms: Experimental Setup

Nine Kiel Off-Shore Mesocosms for future Ocean Simulations (KOSMOS) were deployed in Kongsfjorden (Spitsbergen, Svalbard Archipelago, 78°56.2′N, 11°53.6′E, Figure 1) on 31 May 2010 (day t-7). A detailed description of the experimental setup and sampling procedures is given in *Riebesell et al*. [2013b], *Schulz et al*. [2013], and *Czerny et al*. [2013a]. Briefly, the KOSMOS are enclosures (17 m long and 2 m wide) that are attached to hard floating frames and made of 0.5–1 mm thick thermoplastic polyurethane, which absorbs almost 100% of the incoming UV radiation, while it is transparent to PAR [*Riebesell et al*., 2013b; *Schulz et al*., 2013]. After deployment, enclosures were left open to allow for flushing and after 2 days were closed at the bottom by divers to prevent further exchange with ambient fjord water [*Schulz et al*., 2013]. Each enclosure contained about 45 m^3 of seawater [*Schulz et al*., 2013; *Czerny et al*., 2013a]. To prevent precipitation and airborne contamination, a cap, made of the same material as the enclosures, was set on top of each mesocosm.

©2014. American Geophysical Union. All Rights Reserved.

The whole experimental setup including thermoplastic polyurethane bags has been used in several similar studies over the past years.

The experiment lasted for 31 days from 7 June (day t0) to 7 July (day t30). Fifty kilograms of salt (NaCl) was added to each mesocosm on day t-4 (3 June) and day t4 (11 June) to estimate the exact water volume enclosed in each mesocosm [*Czerny et al*., 2013a]. This was required to calculate the exact amounts of CO_2 and dissolved inorganic nutrients to be added to each mesocosm as experimental treatment [*Schulz et al*., 2013].

pCO_2 inside the mesocosms was gradually increased between days t-1 and t4 by adding CO_2 enriched seawater. Added CO_2-enriched water was injected and evenly dispersed throughout the water column between days t4 and t8 using a device known as the "spider" [*Riebesell et al*., 2013b]. The range of 8 pCO_2 levels averaged for the course of experiment was between 177 ppm and 1084 ppm [*Silyakova et al*., 2013]. Nutrients (5 μmol L^{-1} NO_3^-, 0.32 μmol L^{-1} PO_4^{3-}, and 2.5 μmol L^{-1} $Si(OH)_4$) were added to the enclosures on day t13 to stimulate phytoplankton growth. As there were three peaks of phytoplankton growth, the experiment was divided in three phases: phase I, days t4–t13; phase II, days t14–t21; and phase III, days t22–t27 [*Riebesell et al*., 2013a].

Most seawater samples were collected daily by means of a depth-integrated sampler (5 L) lowered into the mesocosms from the surface to 12 m depth.

2.2. CDOM Sampling and Analysis

Seawater for CDOM analysis was collected during t8–t27 from three out of nine mesocosms, representing mean (for the t8–t27 period) pCO_2 levels of 175 μatm (M3), 600 μatm (M1), and 860 μatm (M5) corresponding to seasonally natural (M3) and elevated (M1, M5) levels of pCO_2. In addition, samples from the fjord surface layer (0–12 m) were taken for comparison. Samples were collected into prewashed 1 L plastic bottles and transported ashore to the Kings Bay Marine Laboratory, Ny-Ålesund. There, samples were filtered through Pall Acrodisc 0.8/0.2 m syringe filters and stored in precombusted amber glass vials at +4°C until analysis.

Absorbance of CDOM was assessed with a standard photometric technique [*Stedmon and Markager*, 2001] using a double beam UV-visible spectrophotometer Shimadzu UV-2450 equipped with a 10 cm quartz cuvette. Ultrapure Milli-Q water was used as a reference. Scans were done in the range of 240–700 nm at 1 nm intervals. Measured absorbance was subsequently converted to absorption coefficients (a, m^{-1}) according to

$$a_{\mathrm{CDOM}}(\lambda) = 2.303 \cdot A_{\mathrm{CDOM}}(\lambda)/L \quad (1)$$

where A is the measured absorbance at wavelength λ, L is the path length of the optical cell in meters (here 0.1 m), and 2.303 is common-to-natural logarithm conversion factor. All spectra were baseline corrected relative to absorption in the range 690–700 nm. The detection level of the spectrophotometer depends on the path length of a used cuvette [*Guéguen and Kowalczuk*, 2013] and is equal to 0.023 m^{-1} in our study.

Spectral slope coefficients (S, nm^{-1}) were calculated for different wavelength bands. S values for the wavelength range 300–650 nm ($S_{300-650}$) were derived from equation (2) using a nonlinear fit (NLF) [*Stedmon and Markager*, 2001]. For shorter intervals 275–295 nm ($S_{275-295}$) and 350–400 nm ($S_{350-400}$), slopes were calculated using a linear regression of the log-transformed absorption spectra following *Helms et al*. [2008]:

$$a_{\mathrm{CDOM}}(\lambda) = a_{\mathrm{CDOM}}(\lambda_0) \cdot e^{-S \cdot (\lambda - \lambda_0)} + K \quad (2)$$

where λ_0 is a reference wavelength and K is an additional background parameter to account for any potential baseline shifts not due to CDOM.

The slope ratio (S_R) was calculated as the ratio of $S_{275-295}$ to $S_{350-400}$ as described by *Helms et al*. [2008]. Total absorption by CDOM in the range 250–450 nm was calculated as the integrated absorption with 1 nm resolution [*Helms et al*., 2008].

2.3. Quantification of Mycosporine-Like Amino Acids (MAAs) in CDOM Absorption Spectra

Distinct elevated CDOM absorption values between 300 and 425 nm with absorption peaks centered between 320 and 370 nm were found in 65% of the samples from the fjord and in 20% of the samples from the mesocosms (Figures 2a and 2b). They are most likely related to a presence of mycosporine-like amino acids (MAAs) [*Řezanka et al*., 2004; *Oren and Gunde-Cimerman*, 2007]. To our knowledge, no thorough method has been proposed to date to quantify MAAs peaks present in CDOM absorption spectra. One approach

©2014. American Geophysical Union. All Rights Reserved.

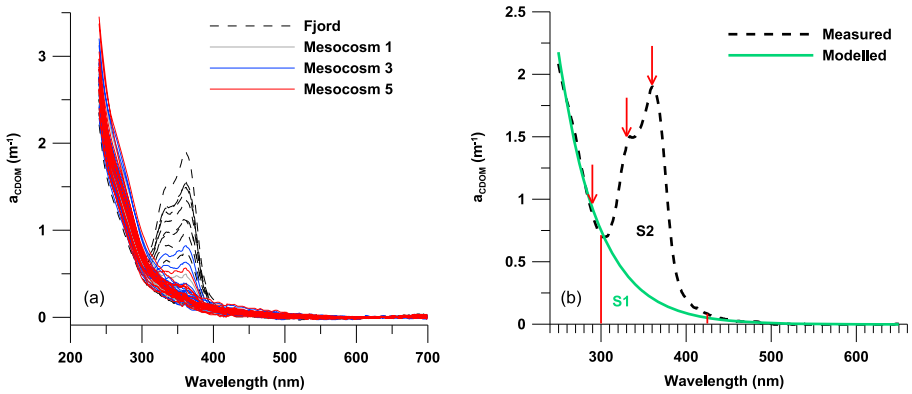

Figure 2. (a) All CDOM absorption spectra from the mesocosms and the fjord ($N = 72$). (b) Example of a CDOM spectrum with a distinct absorption peak from the fjord. Red arrows indicate wavelengths 290, 330, and 360 nm, respectively. S1 and S2 are related to areal MAA index. S1 is an integrated absorption under a modeled spectrum (green curve) in the range 300–425 nm. S2—same for a measured spectrum (black dashed line).

would be to consider simple ratios of CDOM absorption at different wavelengths, e.g., $a_{CDOM}(360)$ (major absorption peak) versus $a_{CDOM}(290)$ (the latter apparently not affected by the absorption peaks) and $a_{CDOM}(330)$ (second major absorption peak) versus $a_{CDOM}(290)$. However, while absorption peaks at 330 nm and 360 nm are most common among MAAs, their magnitude and wavelength location depend on overall MAAs' composition, superposition, and optical properties [*Řezanka et al.*, 2004; *Oren and Gunde-Cimerman*, 2007], so this approach might not be ideal when samples with different MAA composition are considered.

Therefore, we followed another approach to quantify MAAs peaks from CDOM absorption spectra and used it to assess the temporal variability of MAAs under different CO_2 scenarios. We considered all CDOM absorption spectra over the range of 250–650 nm. MAA-like signatures could be identified between 300 and 425 nm (Figure 2b). Therefore, for each spectrum this waveband (300–425 nm) was excluded and a nonlinear exponential fit was applied to estimate the "pure" CDOM spectrum in this waveband (as it would look like in the absence of MAAs) using data for 250–300 nm and 425–650 nm. Then, the integrated absorption under the modeled (S1, Figure 2b) and measured spectra (S2, Figure 2b) was calculated in the range 300 to 425 nm. The difference in area S2–S1 is used as an overall areal index of the presence of MAAs. Using an integrative measure, this approach is intuitively more reliable to describe the MAAs signal, as it is not affected by the potential shift in MAAs absorption peaks due to change in their composition (as would be the case with the first approach).

2.4. Measurements of Other Relevant Parameters Describing the Mesocosm System

Salinity and temperature data were derived from a CTD60M probe (Sea and Sun Technology) (details in *Schulz et al.* [2013]). Concentrations of chlorophyll a and pigment analyses were done by high-performance liquid chromatography (WATERS HPLC with a Varian Microsorb-MV 100-3 C8 column) according to *Barlow et al.* [1997]. DOC samples were analyzed using the high-temperature combustion method (TOC-VCSH, Shimadzu) [*Qian and Mopper*, 1996] (details in *Engel et al.* [2013]). Bacteria and viruses were counted using a bench-top Becton Dickinson FACSCalibur flow cytometer (FCM) equipped with a 488 nm argon laser (details in *Brussaard et al.* [2013]). All data mentioned above are available on Pangaea at http://doi.pangaea.de/10.1594/PANGAEA.769833 [*Svalbard 2010 Team*, 2010].

As measurements of spectral absorption by phytoplankton were not performed, we therefore used an empirical relationship between chl *a*-specific absorption coefficients ($a^*_{ph}(\lambda)$, mg^{-1} m^2) and chl *a* concentration proposed by *Bricaud et al.* [1995]. Then, absorption spectra by phytoplankton for all mesocosms and the fjord were computed based on chl a concentration as follows:

$$a^*_{ph}(\lambda) = A(\lambda) \cdot [chl\ a]^{-B(\lambda)} \tag{3}$$

where $A(\lambda)$ and $B(\lambda)$ are tabulated wavelength-dependent coefficients [*Bricaud et al.*, 1995] and [*chl a*] is the concentration of chl *a* (mg m^{-3}).

©2014. American Geophysical Union. All Rights Reserved.

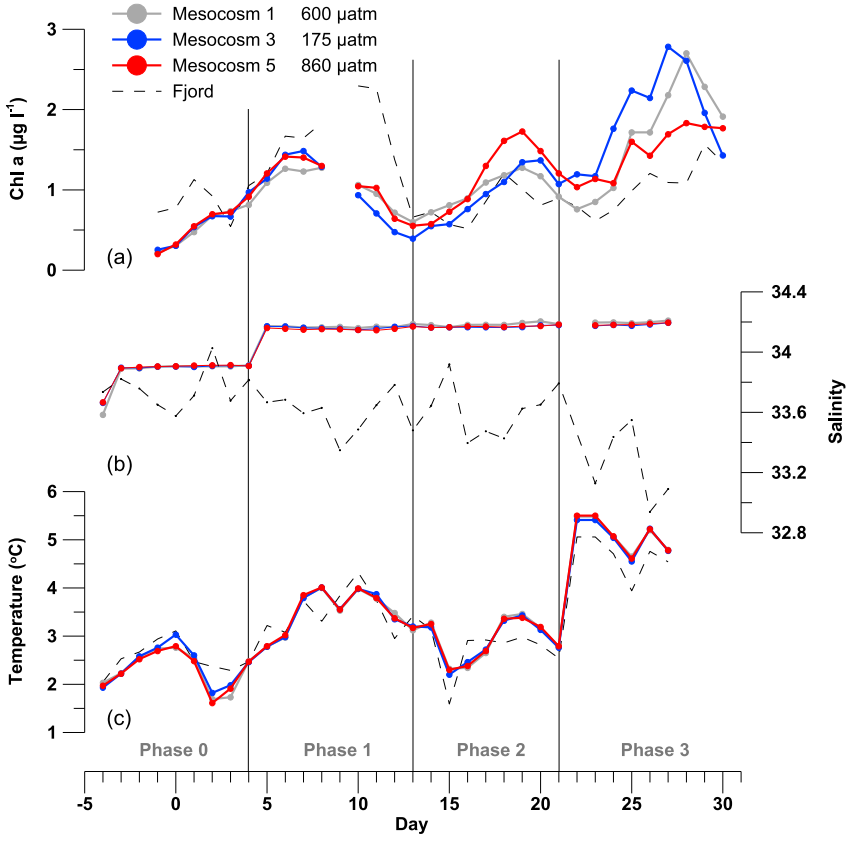

Figure 3. Time series of (a) depth-averaged (0–12 m) chlorophyll a concentration, (b) depth-averaged (0–12 m) sea water salinity, and (c) depth-averaged (0–12 m) sea water temperature.

3. Results

3.1. Changes in Chlorophyll *a*, Salinity, and Temperature

Initial phytoplankton growth in the mesocosms was fueled by nutrients (mostly ammonia) remaining in the fjord after the spring bloom and a second bloom followed the addition of nutrients on day t13 (Figure 3a). Overall phytoplankton development was similar in all mesocosms with chl *a* peaks occurring on days t6–t10 and t16–t19 (both up to 1.5–2.0 µg L^{-1}) and t24–t27 (2.5 µg L^{-1}). In the fjord, chl *a* was more variable without any distinct pattern of variability. For more details on phytoplankton biomass development, see *Schulz et al*. [2013].

Changes in salinity reflect the addition of salt on day t-4 and t4 (see methods), which resulted in a step-like increase in salinity of ~0.3 units each over 1 day in all three mesocosms (Figure 3b). Apart from this, salinity was relatively stable during the experiment and no stratification developed in the mescososms. In contrast, waters in the fjord were stratified [*Schulz et al*., 2013] and salinity of the fjord water had relatively large day-to-day variations and generally decreased during the experimental period. Depth-averaged salinity (0–12 m) varied between 32.94 and 34.03, with a minimum as low as 29.59 at the surface and a maximum of up to 34.29 at 12 m [*Schulz et al*., 2013].

Depth-averaged water temperature in the mesocosms increased during the experiment from ~2°C to ~5°C and mainly followed the temperature of ambient fjord waters (Figure 3c). This warming was mostly pronounced in the upper 5–10 m [*Schulz et al*., 2013].

3.2. Properties of CDOM

To look at CDOM properties, we plotted $S_{300–650}$ against $a_{CDOM}(375)$ for samples from three mesocosms and compared our data (Figure 4) with a model by *Stedmon and Markager* [2001] (SM01) for marine CDOM developed

©2014. American Geophysical Union. All Rights Reserved.

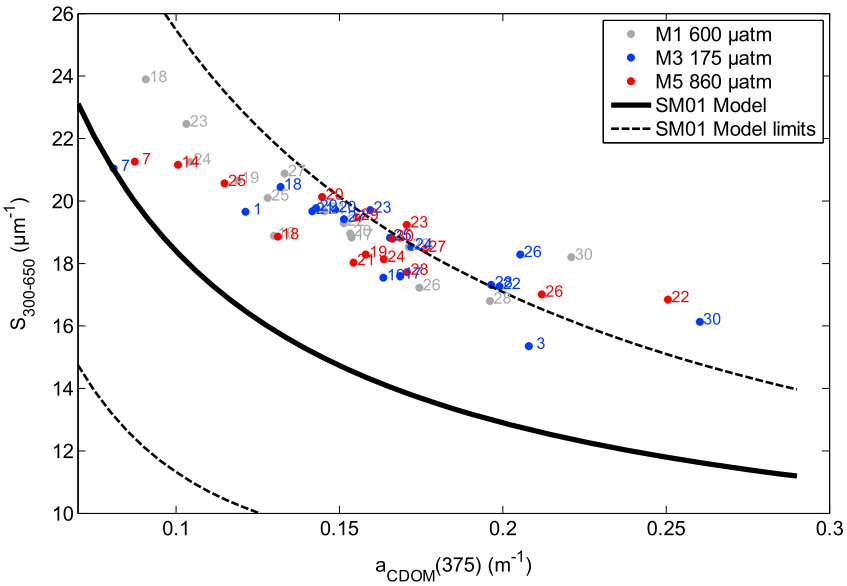

Figure 4. $S_{300-650}$ against $a_{CDOM}(375)$. Thick line is a model of *Stedmon and Markager* [2001] for marine CDOM with corresponding model limits (thin dashed line). Labels indicate the day of the experiment when samples were collected.

for the Greenland Sea. Only spectra without MAA-like features were used. Values of $a_{CDOM}(375)$ ranged between 0.07 and 0.27 m^{-1}, while $S_{300-650}$ varied from 16 to 24 µm^{-1}. No apparent differences between mesocosms were found. A majority of observations were within model limits, particularly in the beginning of the experiment.

Excluding absorption spectra with MAA-like features, $S_{275-295}$ was similar between mesocosms (26.8–27.0 µm^{-1}), while $S_{350-400}$ were different (18.9–23.5 µm^{-1}). In the fjord, both $S_{275-295}$ and $S_{350-400}$ were higher than in mesocosms (Table 1). The slope ratio (S_R) of $S_{275-295}$ to $S_{350-400}$ exceeded 1.0 and ranged between 1.20 and 1.42. Average values for S_R were 1.42, 1.20, and 1.38 for mesocosms 3, , and 5, respectively, and 1.26 for the fjord.

Average DOC concentrations varied between 85 and 90 µmol L^{-1} in the mesocosms and were close to 75 µmol L^{-1} in the fjord.

MAA-like absorption peaks were found in all mesocosms, mainly during the first phase of the experiment, although the magnitude of these peaks slightly differed between mesocosms. In the fjord, MAA-like peaks in absorption spectra were considerably higher and did not match with MAA occurrence in mesocosms (Figure 5c).

3.3. Dynamics of CDOM and Other Relevant Parameters Throughout the Experiment

3.3.1. CDOM Absorption

Generally, absorption by CDOM was comparatively low in the study area. Therefore, we used absorption coefficients at 295 nm ($a_{CDOM}(295)$) as a measure of CDOM concentration during the experiment (Figure 5a).

Table 1. Average Spectral Properties of CDOM in Three Mesocosms and the Fjord[a]

	Mesocosm 1	Mesocosm 3	Mesocosm 5	Fjord
A(295) ± SD	0.7543 ± 0.1013^{A}	0.7840 ± 0.1215^{B}	0.7838 ± 0.1354^{C}	$0.6783 \pm 0.0826^{A,B,C}$
A(254) ± SD	1.8528 ± 0.1398	1.9114 ± 0.1957	1.9508 ± 0.2265^{A}	1.7926 ± 0.1401^{A}
$S_{275-295}$ ± SD	26.8 ± 1.9^{A}	26.8 ± 1.7^{B}	27.0 ± 2.2^{C}	$30.1 \pm 1.9^{A,B,C}$
$S_{350-400}$ ± SD	23.5 ± 6.8^{B}	$18.9 \pm 2.5^{A,B}$	20.2 ± 6.3	24.9 ± 5.5^{A}
S_R ± SD	1.1964 ± 0.3012^{A}	1.4180 ± 0.1831^{A}	1.3846 ± 0.2742	1.2619 ± 0.2075
DOC ± SD	90.5655 ± 10.3077^{A}	85.3150 ± 11.3059^{B}	88.2747 ± 10.5259^{C}	$74.5098 \pm 11.7545^{A,B,C}$
Total a ± SD	96.2665 ± 10.3172^{A}	102.1394 ± 13.8105^{B}	102.3969 ± 15.7846^{C}	$79.4803 \pm 8.2122^{A,B,C}$

[a]Mean and standard deviations for absorption by CDOM at 254 and 295 nm, CDOM absorption spectra slopes for ranges 275–295 and 350–400 nm, spectral slope ratio (S_R), concentration of DOC, and total CDOM absorption in the range 250–450 nm. Superscripts A, B, and C indicate significantly different means ($p = 0.05$, t test).

©2014. American Geophysical Union. All Rights Reserved.

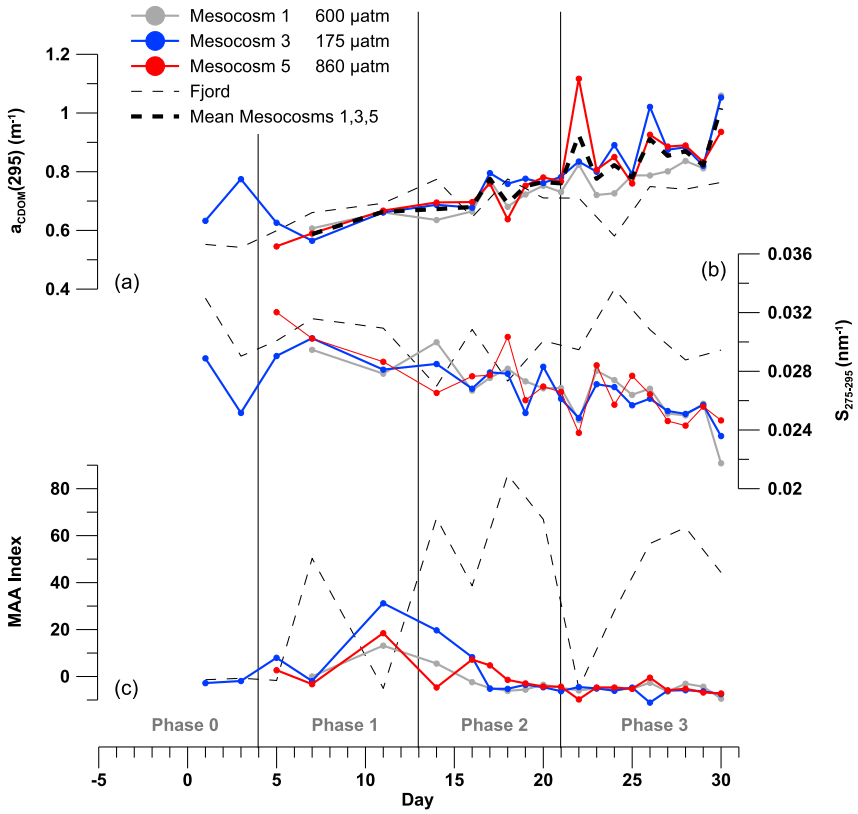

Figure 5. Time series of (a) absorption coefficients by CDOM ($a_{CDOM}(295)$), (b) CDOM absorption spectra slopes ($S_{275-295}$), and (c) MAA index.

This wavelength was also chosen because it is unaffected by MAA-like absorption features. $a_{CDOM}(295)$ steadily increased in all three experimental mesocosms. On day t7, values of $a_{CDOM}(295)$ were similar in all three studied mesocosms (0.56 m^{-1}, 0.61 m^{-1}, and 0.59 m^{-1}, for mesocosms 3, 1, and 5 respectively). By the end of the experiment (day t30), $a_{CDOM}(295)$ reached 1.05 m^{-1}, 1.06 m^{-1}, and 0.94 m^{-1}, respectively. Linear trends for the period between t7 and t30 were found to be statistically significant at $p < 0.05$ (Table 2). Lowest trends were found in mesocosms 1 (0.0128 ± 0.0024 m^{-1} d^{-1}) and 5 (0.0144 ± 0.0034 m^{-1} d^{-1}) with highest pCO2 levels, while highest CDOM absorption increase took place in the control mesocosm 3 (0.0163 ± 0.0023 m^{-1} d^{-1}) with a background (natural) level of pCO_2 (Table 1). For comparison, evolution of $a_{CDOM}(295)$ in fjord waters is also shown in Figure 5a. There, $a_{CDOM}(295)$ was more variable and slightly increased during the experiment, but without a significant trend ($p > 0.05$). Total absorption in the range 250–450 nm varied between ~96 and ~102 in the mescososms and was ~80 in the fjord, which indicate that relatively low CDOM absorption during the experiment.

3.3.2. Slopes of CDOM Absorption Spectra

Time series of $S_{275-295}$ were consistent and similar between mesocosms. In the beginning of the experiment (t7), $S_{275-295}$ in all three mesocosms were almost equal with 30.25, 29.46, and 30.22 μm^{-1} for mesocosms 3, 1,

Table 2. Accumulation of $a_{CDOM}(295)$ (m^{-1} d^{-1}) and Change in $S_{275-295}$ (μm^{-1} d^{-1}) in the Mesocosms[a]

	N	$a_{CDOM}(295) \pm SE$	R^2	$S_{275-295} \pm SE$	R^2
M1	18 (t7–t30)	0.0128 ± 0.0024	0.65	-0.224 ± 0.049	0.54
M3	18 (t7–t30)	0.0163 ± 0.0023	0.75	-0.214 ± 0.037	0.66
M5	18 (t7–t30)	0.0144 ± 0.0034	0.52	-0.208 ± 0.053	0.46
Mean	18 (t7–t30)	0.0145 ± 0.0021	0.75		

[a]All trends are significant at $p < 0.01$.

©2014. American Geophysical Union. All Rights Reserved.

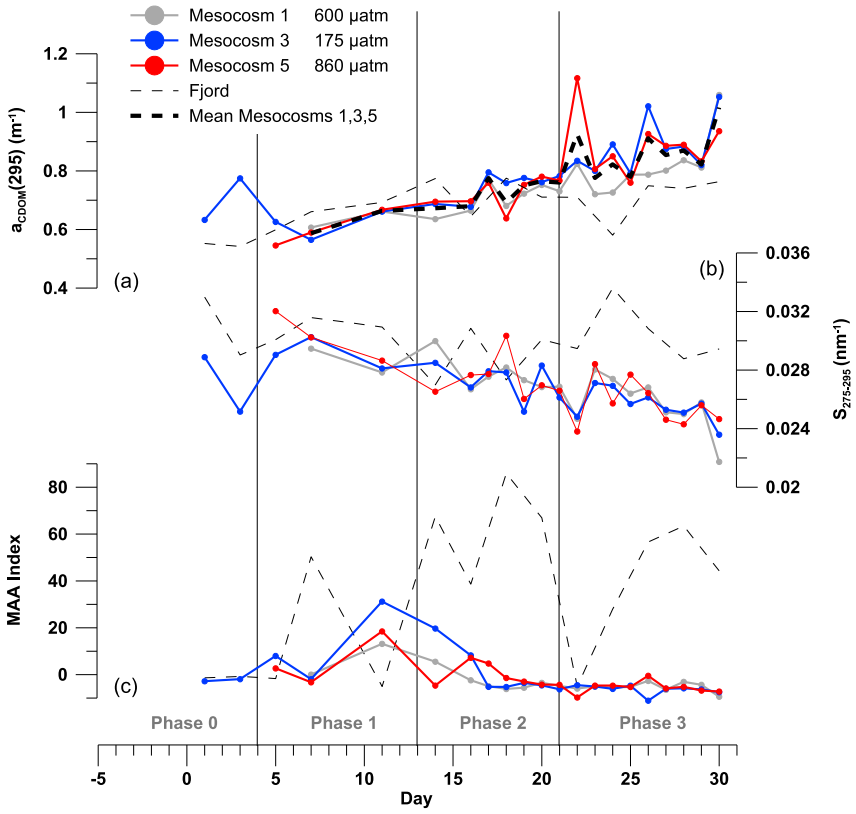

Figure 6. Time series of (a) DOC concentration, (b) total bacteria abundance, and (c) total viral abundance.

and 5, respectively. At the end of the experiment (day t30), $S_{275-295}$ reached 23.59, 21.73, and 24.65 μm^{-1} in corresponding mesocosms. Linear trends estimated for the period between t7 and t30 were found to be statistically significant at $p < 0.01$. Estimated trend values were -0.214 ± 0.037, -0.224 ± 0.049, and -0.208 ± 0.053 μm^{-1} d^{-1} (Table 2). As in case with $a_{CDOM}(295)$, variability of $S_{275-295}$ in a fjord was much higher, and $S_{275-295}$ values were generally higher than in the mesocosms (Figure 5b).

3.3.3. MAAs

In the mesocosms, the development of the MAA index was very coherent (Figure 5c), with distinct peaks in the first phase and in the beginning of a second phase of the experiment (days t6–t16) in with generally comparable magnitude between mesocosms and slightly higher peak in mesocosm 3. After day t19, the MAA index in all three mesocosms was close to or slightly below zero, corresponding to an absence of MAA-like features in CDOM absorption spectra. In the fjord, MAA index was more variable and reached values twice as high as compared to mesocosms.

3.3.4. DOC

DOC concentration ranged between 70 and 115 $\mu mol\ L^{-1}$. Considerable day-to-day variations of up to 30% were observed in both fjord and mesocosms (Figure 6a). Based on data from all nine mesocosms, *Engel et al.* [2013] showed that DOC increased significantly until nutrient addition; however, this may not be apparent from three mesocosms considered here. At the same time, *Engel et al.* [2013] suggested that this might be attributed to contamination of samples during sample collection, transport, or instrument deployment. For this reason, we did not estimate trends in DOC concentration but used average DOC values (over the course of experiment) for interpretation of other results assuming that potential methodological errors occurred randomly [*Engel et al.*, 2013]. Visually, there was no clear pattern of variability in all three studied mesocosms. DOC concentrations in the fjord had slightly larger variability compared to mesocosms.

3.3.5. Bacteria and Viruses

Total bacterial and viral abundances increased overall during the experiment in all mesocosms (Figures 6c and 6d). At the end of experiment, total bacteria exceeded 4.4×10^6 cells ml^{-1}, while total viruses reached 1.6×10^8 cells ml^{-1}. For bacteria, there was an apparent inverse relationship between pCO_2 treatment

©2014. American Geophysical Union. All Rights Reserved.

and abundance of bacteria during second half of experiment. Abundances of bacteria and viruses in the fjord were relatively low and did not exceed 2.0×10^6 cells ml^{-1} and 6.0×10^7 cells ml^{-1}, respectively. More thorough description of bacterial and viral communities during the experiment can be found in *Brussaard et al.* [2013].

4. Discussion

4.1. Properties and Origin of CDOM During Experiment

In summer, water mass structure in Kongsfjorden is to a large extent influenced by river runoff and glacial melt forming a surface brackish layer [*Svendsen et al.*, 2002]. Vegetation is relatively poor on Svalbard, and therefore, organic matter (including CDOM) delivery from land is low [*Johansen and Tømmervik*, 2013], especially in comparison with large Arctic rivers [e.g., *Stedmon et al.*, 2011]. Figure 3 confirms this assumption, showing that a cluster of samples in the beginning of experiment (with lowest $a_{CDOM}(375)$) sits within the limits of the SM01 model for marine CDOM. This CDOM was either biologically produced within a fjord or was advected from adjacent waters before the experiment. In case of terrestrial CDOM, data points would distribute toward higher absorption values with relatively constant slope values [e.g., see *Granskog*, 2012, Figure 4]. Apart from the original study by *Stedmon and Markager* [2001] in the southern part of the Greenland Sea, this empirical model was also successfully applied to distinguish between marine and terrestrial CDOM in Fram Strait [*Granskog et al.*, 2012], adjacent to Kongsfjorden. This leads us to conclude that CDOM observed in mesocosms was of autochthonous origin and therefore potentially labile and available for further utilization and turnover [*Nelson and Siegel*, 2002] within the experimental ecosystems.

Toward the end of the experiment some data points drifted out of the SM01 model limits. There was no water exchange with ambient fjord waters, suggesting that these signatures (nonmarine-looking) were produced inside experimental mesocosms. Indeed, previous studies in temperate waters observed production of humic-like substances by marine phytoplankton [e.g., *Romera-Castillo et al.*, 2010]. As was stressed earlier, marine ecosystems of the Arctic Ocean are typically dominated by high terrestrial CDOM that mask marine CDOM, making it difficult to study its properties in isolation. In this case, for the first time to our knowledge, we report about signatures of apparently humic-like substances produced in situ in an Arctic marine ecosystem.

Helms et al. [2008] proposed that absorption spectral slopes ($S_{275-295}$ and $S_{350-400}$) and especially their slope ratio (S_R) can serve as a good proxy of a molecular weight and a source of CDOM. During this experiment, average S_R values exceeded 1.0, and according to *Helms et al.* [2008], S_R values higher than 1.0 are typical for marine CDOM opposed to high molecular CDOM of terrestrial samples with S_R below 1.0.

There was no apparent relationship between $a_{CDOM}(295)$ and DOC concentrations in three mesocosms (not shown). While CDOM is essentially a part of the DOC pool, different mechanisms are responsible for production and removal of both DOC and CDOM. For example, photobleaching could influence CDOM compounds significantly without altering DOC concentrations. Therefore, a strong relationship between CDOM and DOC may not exist for the open ocean, dominated by marine autochtonously produced CDOM [cf. *Siegel et al.*, 2002; *Rochelle-Newall et al.*, 2014]. In contrast, in areas strongly influenced by inputs of terrestrial dissolved organic matter, significant positive relationships have been found between CDOM and DOC [e.g., *Spencer et al.*, 2009; *Fichot and Benner*, 2012]. Thus, this further indicates that CDOM present in the mesocosms during the experiment was of marine origin and was not controlled by terrestrial organic matter.

4.2. Dynamics of CDOM

In general, evolution of a CDOM pool in the water column is defined by the balance between in situ CDOM production and degradation, advection, and removal [*Nelson and Siegel*, 2002]. In a closed mesocosm experiment, one could expect that processes such as in situ production and microbial alteration would play a central role in a dynamics of CDOM. We believe that processes of CDOM photobleaching that are certainly relevant in the ocean surface layer did not contribute to a change in CDOM in mesocosms because of the very limited transmittance of UV light by the mesocosm walls and roofs [*Riebesell et al.*, 2013b; *Schulz et al.*, 2013].

Estimates of linear regression slope coefficients of $a_{CDOM}(295)$ accumulation with corresponding standard errors overlapped between mesocosms, thus indicating no significant effect of elevated pCO_2 on CDOM accumulation. Taking this into account, a mean trend was also estimated for all three mesocosms with a

©2014. American Geophysical Union. All Rights Reserved.

value of 0.0145 ± 0.0021 m^{-1} d^{-1} (Table 2) showing a general accumulation of CDOM throughout the experiment (Figure 5a).

Earlier studies on autochthonous CDOM production in aquatic systems suggested a number of mechanisms through which CDOM can be produced in situ. These include processing of organic matter into CDOM by bacteria [*Nelson et al*., 1998, 2004; *Rochelle-Newall et al*., 1999; *Steinberg et al*., 2004], excretion from zooplankton [*Steinberg et al*., 2004], lysis of heterotrophic bacteria by viruses [*Balch et al*., 2002; *Lønborg et al*., 2013], release by phytoplankton [*Vernet and Whitehead*, 1996; *Rochelle-Newall and Fisher*, 2002], and phytoplankton degradation [cf. *Zhang et al*., 2011]. All findings from these studies come from tropical or temperate marine environments or freshwater ecosystems. In this regard, information on properties and dynamics of freshly produced marine CDOM from a high-latitude ecosystem is rare and contributes to the general knowledge on CDOM dynamics in aquatic systems.

The initial gradual increase in $a_{CDOM}(295)$ was not influenced by two peaks of phytoplankton biomass as indicated by chl *a*, and no correlation between them was found. The gradual accumulation of CDOM was not accompanied by an increase in DOC, which slightly increased until day t15 [*Engel et al*., 2013]. However, there was a slight increase in DOC found toward the end of the experiment based on carbon budget estimations by *Czerny et al*. [2013b]. Earlier, *Rochelle-Newall et al*. [2004] observed neither significant CDOM nor DOC accumulation under various pCO_2 treatments during similar mesocosm experiment in a temperate fjord off Bergen, Norway (60.3 N).

Possible difference in CDOM accumulation between the present study and a study performed by *Rochelle-Newall et al*. [2004] can be possibly explained by differences of the studied ecosystems. Kongsfjorden is known to have a very efficient heterotrophic microbial loop [*Iversen and Seuthe*, 2011; *Seuthe et al*., 2011], while the ecosystem studied by *Rochelle-Newall et al*. [2004] was more autotrophic as concentrations of chl *a* were of an order of magnitude higher and bacteria abundances were few times lower during Bergen experiment compared to Kongsfjorden. Increase in $a_{CDOM}(295)$ in all mesocosms follows closely a gradual increase in the abundance of bacteria. We found significant positive correlation coefficients (R) between $a_{CDOM}(295)$ and total bacteria in mesocosms 1 and 3 (0.904 and 0.975, $p < 0.05$). For mesocosm 5, correlation coefficient between $a_{CDOM}(295)$ and total bacteria was 0.743 ($p > 0.05$). Total viral abundance also gradually increased during the experiment. However, significant correlation with $a_{CDOM}(295)$ was not found for any of the mesocosms. Therefore, we deduce that in situ CDOM accumulation in all three mesocosms was likely related to the enhanced microbial activity in the studied Arctic ecosystem, which is consistent with previous studies on CDOM production by bacteria [*Nelson et al*., 1998, 2004; *Rochelle-Newall et al*., 1999; *Steinberg et al*., 2004].

Bacterial abundances simultaneously increased in all mesocosms toward the end of the experiment. While it was not largely different between mesocosms during the first phase of the experiment, there was a clear trend toward less bacteria abundance under high pCO_2 levels [see also *Brussaard et al*., 2013]. Highest abundance of bacteria in mesocosm 3 is consistent with slightly higher increase in CDOM in the same mesocosm (Table 2). Despite the lack of evidence of different responses of CDOM to varying pCO_2 treatments, an overall accumulation of CDOM (0.0145 ± 0.0021 m^{-1} d^{-1}) is contrary to previous mesocosm studies [*Rochelle-Newall and Fisher*, 2002; *Rochelle-Newall et al*., 2004].

During our experiment, levels of UV irradiance were negligible in mesocosms, and no photobleaching at shorter wavelengths (<400 nm) can be expected. *Helms et al*. [2008] found different effects of irradiation and microbial activity on spectral absorption slopes of CDOM. In their study, in contrast to an increase in $S_{275-295}$ due to irradiation, microbial processes (microbial production or preservation long-wavelength absorbing substances) led to a decrease in S_R (which is proportional to $S_{275-295}$). Therefore, this further suggests that the decrease in $S_{275-295}$ in the course of the experiment is related to microbial activity being largely responsible for CDOM dynamics during the experiment. In contrast $S_{275-295}$ in the fjord did not change and was higher than in the mesocosms at the end of the experiment, which in turn could indicate a contribution of photobleaching to the CDOM dynamics there. This could be partly caused by stronger stratification in the fjord.

4.3. MAA Signatures in CDOM Absorption Spectra

MAAs are secondary metabolites and as low-molecular weight water-soluble molecules have previously been detected on CDOM or particulate absorption spectra by the presence of local absorption maxima in the ultraviolet (UV) band, between 310 and 360 nm [*Whitehead and Vernet*, 2000]. Due to these properties, they

©2014. American Geophysical Union. All Rights Reserved.

have been known for a long time as photoprotective compounds [*Řezanka et al*., 2004; *Oren and Gunde-Cimerman*, 2007; *Uusikivi et al*., 2010]. Recently, more evidence has been collected for the MAAs to be rather multipurpose secondary metabolites that are produced in response to various external stressors such as UV light exposure, desiccation, thermal and salt (osmotic) stress, and other stressors [cf. *Oren and Gunde-Cimerman*, 2007].

For the first time to our knowledge, we described MAA signatures in CDOM absorption spectra in Arctic waters, likely due to the absence of a strong terrigenous or humic-like CDOM pool in the experimental area that may usually mask these or make production of these compounds redundant. Observed coherent peaks in the MAA index during phase 1 and beginning of phase 2 suggest that they were caused either by an external forcing or a common internal forcing or manipulation within all mesocosms. Since the mesocosm setup did not transmit UV radiation ($<$400 nm), UV light exposure cannot be considered as a contributor to increased MAAs in the mesocosms; thus, other mechanisms had to contribute.

MAAs production due to thermal stress was previously reported in tropical waters [*Michalek-Wagner*, 2001]. An increase in water temperature in the first phase of the experiment coincided with higher values of MAA index. However, further changes in water temperature did not match with changes in the MAA index, which was constant at the end of phase 2 and during phase 3. So, it is difficult to conclude that warming of the water in mesocosms induced the MAA signatures.

Salt additions on days t-4 and t4 and subsequent step-like increase in salinity could potentially contribute to an observed simultaneous increase in MAAs in all mesocosms. This would be consistent with previous reports on intracellular MAAs production as additional osmotic solutes in response to ambient salinity increase [*Oren*, 1997]. However, the change in salinity is quite small, only about 1%; thus, it is unlikely that such a change would affect physiology of microorganisms.

In the fjord, with an increased stratification in the upper 5–10 m and natural UV exposure, MAA index was significantly higher than in mesocosms, thus confirming that MAAs are produced under elevated UV light levels. Also, the higher $S_{275-295}$ values point to higher exposure in the fjord (see above). This is consistent with *Ha et al*. [2012] who investigated MAAs produced by phytoplankton in response to UV exposure.

Ha et al. [2012] also considered the chemical composition of MAAs in Kongsfjorden earlier. Based on laboratory analyses, five different types of MAAs (shinorine, palythine, mycosporine-glycine, porphyra-334, and asterina-330) were identified in surface waters of Kongsfjorden in late May 2009. Wavelengths of their (5 MAAs) maximum absorption ranged between 310 and 334 nm. In the present study, primary peaks were centered around 360 nm. This indicates that contributions from other MAAs with an absorption maximum around this wavelength are likely to dominate. Among MAAs known from the literature, palythene and usujirene have absorption peaks at 360 nm and 357 nm [*Řezanka et al*., 2004], and we surmise that they could account for the primary absorption peak at 360 nm in both fjord and mesocosms.

The MAA index introduced in this study does not describe the chemical composition of MAAs. However, in the future, established empirical relationships between the proposed MAA absorption index and MAAs concentrations (total and individual) may provide a relatively easy quantitative measure of MAA compounds compared to demanding high-performance liquid chromatography (HPLC) measurements of MAAs concentrations [*Řezanka et al*., 2004]. Production and presence of MAA-like absorption signatures in mesocosms shows that MAAs can be produced in a high-latitude ecosystem in response to stressors other than UV radiation alone.

4.4. Contribution of CDOM and Phytoplankton to Spectral Absorption in a PAR Range—Implications for Phytoplankton Ecology

Over decades, PAR integrated over 400–700 nm has been widely used in biological and ecological studies [*Behrenfeld and Falkowski*, 1997]. Though, especially with recent advances in instrumentation, it is essential to look at light spectrally and use spectral light photosynthesis models in applications to marine photosynthesis [e.g., *Lehmann et al*., 2004].

We used an empirical relationship to simulate absorption spectra by phytoplankton [*Bricaud et al*., 1995]. This relationship does not describe the spectral absorption properties of different phytoplankton groups but at the same time provides insight to the general trend of spectral absorption by phytoplankton with a

©2014. American Geophysical Union. All Rights Reserved.

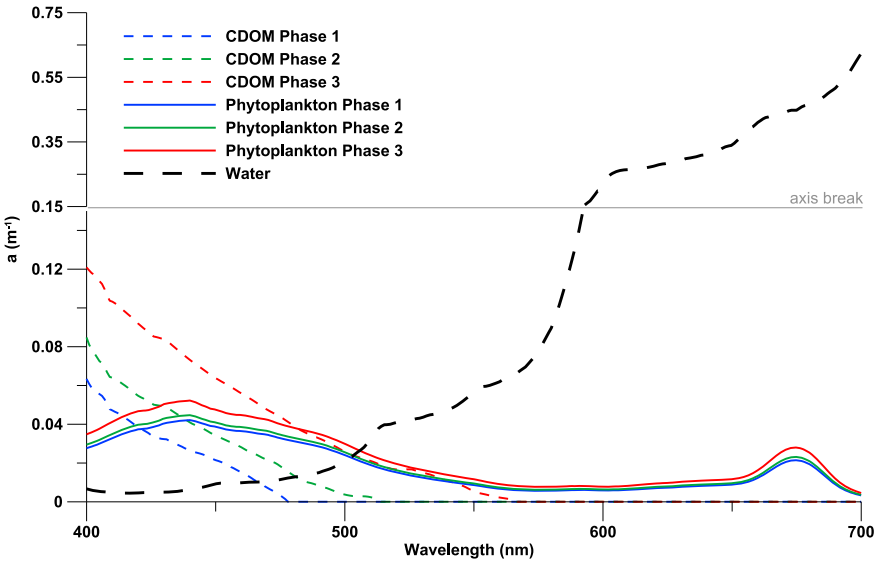

Figure 7. Absorption spectra of CDOM, phytoplankton, and pure water in mesocosm 5 for three stages of the experiment.

possibility to compare it with the magnitude of CDOM absorption observed during the experiment (Figure 7). The spectral absorption coefficient by pure water [*Pope and Fry*, 1997] dominates the absorption in the PAR range due to high absorption at longer wavelengths (see Figure 7).

Furthermore, to stress the importance of considering spectral light absorption, we estimated relative contributions from CDOM, phytoplankton, and seawater to total absorption at a wavelength of 440 nm, which corresponds to maximum phytoplankton absorption (Figure 7) [e.g., *Ciotti et al*., 2002]. This estimate was made separately for the three phases of the experiment (figure not shown). In all three mesocosms, an increase in CDOM absorption throughout the experiment led to a shift in relative contribution to total absorption at 440 nm. During phase 1, phytoplankton was the major contributor to the total absorption at 440 nm (55–62%). Contribution of CDOM ranged between 32 and 37%. By the end of experiment (phase 3), CDOM clearly dominated the absorption (mesocosms 3 and 5) or was comparable to phytoplankton (mesocosm 1). In the fjord, the situation was different and phytoplankton dominated the total absorption during the whole experiment, in the absence of CDOM accumulation.

With this example, we demonstrate that even a slight increase in CDOM absorption can alter spectral underwater light availability in the wavelength region of utilization of light by phytoplankton and, therefore, can potentially increase competition between different phytoplankton groups, promote photoacclimation processes, and inhibit development of some phytoplankton species that utilize light at shorter wavelengths.

5. Conclusions

Our study is one of the first on marine CDOM that is typically masked by significantly higher concentrations of terrestrially borne CDOM in the Arctic Ocean. Although according to the empirical model of *Stedmon and Markager* [2001], at the beginning of the experiment CDOM had typical marine properties, toward the end of the experiment a nonmarine-like signatures of CDOM were apparently formed. We found significant CDOM accumulation, which contrasts findings in a previous similar experiment in temperate waters [*Rochelle-Newall and Fisher*, 2002; *Rochelle-Newall et al*., 2004]. However, no significant response of CDOM accumulation to different pCO_2 treatments was found. CDOM accumulation was in line with an increase in bacterial abundance in the mesocosms. Temporal changes in CDOM spectral slopes also indicate that bacteria were most likely responsible for the observed CDOM dynamics.

CDOM absorption spectra had frequently peaks of elevated absorption in the range from 300 to 425 nm, typical of so-called mycosporine-like amino acids (MAAs). For the first time to our knowledge, we introduced a simplistic areal MAA absorption index to describe MAAs peaks in CDOM absorption spectra. By analyzing the MAA index, we found a distinct difference between CDOM properties in the fjord and in the mesocosms.

©2014. American Geophysical Union. All Rights Reserved.

MAA signatures in the mesocosms were produced in the absence of UV exposure (blocked by mesocosm walls), providing another indication that MAAs act not only as photo protective compounds, but are multipurpose metabolites [*Oren and Gunde-Cimerman*, 2007].

We examined closer the spectral absorption by CDOM, phytoplankton, and pure water and modeled their relative contribution to total absorption at 440 nm corresponding to a wavelength of maximum phytoplankton absorption. Based on calculations, even the small increase in CDOM could be important for spectral light availability and competition for light among different phytoplankton groups and therefore is important for photosynthesis. It is essential to consider this in the future summer ice free Arctic marine ecosystem.

Acknowledgments

This work is a contribution to the "European Project on Ocean Acidification" (EPOCA) which received funding from the European Commission's Seventh Framework Program (FP7/2007–2013) under grant agreement 211384. We gratefully acknowledge the logistical support of Greenpeace International for its assistance with the transport of the mesocosm facility from Kiel to Ny-Ålesund and back to Kiel. We also thank the captains and crews of M/V *Esperanza* of Greenpeace and R/V *Viking Explorer* of the University Centre in Svalbard (UNIS) for assistance during mesocosm transport and during deployment and recovery in Kongsfjorden. We thank the staff of the French-German Arctic Research Base at Ny-Ålesund, in particular Marcus Schumacher, for on-site logistical support. We thank Gisle Nondal for help with sampling. This work was also supported by the Centre for Ice, Climate and Ecosystems (ICE) at the Norwegian Polar Institute. For A.K.P., this study was partially supported by the Russian Foundation for Basic Research (RFBR), research project 12-05-00780_a and 14-05-10065, Roshydromet project 1.5.3.3, President Grant MK-4049.2014.8, and the joint AARI-NPI Fram Arctic Climate Research Laboratory. M.A.G. and A.K.P. research work has partially received funding from the Polish-Norwegian Research Programme operated by the National Centre for Research and Development under the Norwegian Financial Mechanism 2009–2014 in the frame of Project Contract Pol-Nor/197511/40/2013, CDOM-HEAT. For R.G.J.B., the work was partially funded by the project Marine Ecosystem Response to a Changing Climate (MERCLIM 184860) financed by the program NORKLIMA through the Norwegian Research Council, "Marine Ecosystem Evolution in a Changing Environment" (MEECE 212085), "Basin-scale Analysis, Synthesis and Integration" (EURO-BASIN 26493), and "Development of global plankton data base and model system for ecoclimate early warning" (Greenseas 265294). We thank Dmitry Divine and Piotr Kowalczuk for valuable discussions and comments. All data used in this paper (except CDOM data) are available on Pangaea at http://doi.pangaea.de/10.1594/PANGAEA.769833. The CDOM data are available upon request from the authors.

References

Arctic Monitoring and Assessment Programme (AMAP) (2011), Snow, water, ice and permafrost in the Arctic (SWIPA) Arctic Monitoring and Assessment Programme (AMAP), Oslo, Norway.

Arctic Monitoring and Assessment Programme (AMAP) (2013), AMAP assessment 2013: Arctic ocean acidification Arctic Monitoring and Assessment Programme (AMAP), Oslo, Norway, viii + 99 pp.

Arctic Climate Impact Assessment (2005), *Impacts of a Warming Arctic-Arctic Climate Impact Assessment Overview Report*, Cambridge Univ. Press, New York.

Arrigo, K. R., G. van Dijken, and S. Pabi (2008), Impact of a shrinking Arctic ice cover on marine primary production, *Geophys. Res. Lett.*, *35*, L19603, doi:10.1029/2008GL035028.

Balch, W. M., J. M. Vaughn, J. F. Novotny, D. T. Drapeau, J. I. Goes, E. Booth, J. M. Lapierre, C. L. Vining, and A. Ashe (2002), Fundamental changes in light scattering associated with infection of marine bacteria by bacteriophage, *Limnol. Oceanogr.*, *47*(5), 1554–1561.

Barlow, R. G., D. G. Cummings, and S. W. Gibb (1997), Improved resolution of mono-and divinyl chlorophylls a and b and zeaxanthin and lutein in phytoplankton extracts using reverse phase C-8 HPLC, *Mar. Ecol. Progr. Ser.*, *161*, 303–307.

Behrenfeld, M. J., and P. G. Falkowski (1997), A consumer's guide to phytoplankton primary productivity models, *Limnol. Oceanogr.*, *42*(7), 1479–1491.

Bélanger, S., M. Babin, and J.-É. Tremblay (2013), Increasing cloudiness in Arctic damps the increase in phytoplankton primary production due to sea ice receding, *Biogeosciences*, *10*, 4087–4101, doi:10.5194/bg-10-4087-2013.

Blough, N. V., and R. Del Vecchio (2002), Chromophoric DOM in the coastal environment, in *Biogeochemistry of Marine Dissolved Organic Matter*, edited by, edited by D. A. Hansell and C. A. Carlson, pp. 509–546, Academic Press, San Diego.

Bricaud, A., A. Morel, and L. Prieur (1981), Absorption by dissolved organic matter of the sea (yellow substance) in the UV and visible domains, *Limnol. Oceanogr.*, *26*(1), 43–53.

Bricaud, A., M. Babin, A. Morel, and H. Claustre (1995), Variability in the chlorophyll-specific absorption coefficients of natural phytoplankton: Analysis and parameterization, *J. Geophys. Res.*, *100*(C7), 13,321–13,332, doi:10.1029/95JC00463.

Brussaard, C. P. D., A. A. M. Noordeloos, H. Witte, M. C. J. Collenteur, K. Schulz, A. Ludwig, and U. Riebesell (2013), Arctic microbial community dynamics influenced by elevated CO2 levels, *Biogeosciences*, *10*, 719–731, doi:10.5194/bg-10-719-2013.

Ciotti, A. M., M. R. Lewis, and J. J. Cullen (2002), Assessment of the relationships between dominant cell size in natural phytoplankton communities and the spectral shape of the absorption coefficient, *Limnol. Oceanogr.*, *47*(2), 404–417.

Czerny, J., K. G. Schulz, A. Ludwig, and U. Riebesell (2013a), Technical note: A simple method for air-sea gas exchange measurements in mesocosms and its application in carbon budgeting, *Biogeosciences*, *10*, 1379–1390, doi:10.5194/bg-10-1379-2013.

Czerny, J., et al. (2013b), Implications of elevated CO2 on pelagic carbon fluxes in an Arctic mesocosm study—An elemental mass balance approach, *Biogeosciences*, *10*(5), 3109–3125, doi:10.5194/bg-10-3109-2013.

Dittmar, T., and G. Kattner (2003), The biogeochemistry of the river and shelf ecosystem of the Arctic Ocean: A review, *Mar. Chem.*, *83*(3), 103–120, doi:10.1016/S0304-4203(03)00105-1.

Engel, A., C. Borchard, J. Piontek, K. G. Schulz, U. Riebesell, and R. Bellerby (2013), CO2 increases 14C primary production in an Arctic plankton community, *Biogeosciences*, *10*, 1291–1308, doi:10.5194/bg-10-1291-2013.

Fichot, C., and R. Benner (2012), The spectral slope coefficient of chromophoric dissolved organic matter ($S_{275-295}$) as a tracer of terrigenous dissolved organic carbon in river-influenced ocean margins, *Limnol. Oceanogr.*, *57*, 1453–1466.

Gibson, J. A., W. F. Vincent, B. Nieke, and R. Pienitz (2000), Control of biological exposure to UV radiation in the Arctic Ocean: Comparison of the roles of ozone and riverine dissolved organic matter, *Arctic*, *53*(4), 372–382.

Granskog, M. A. (2012), Changes in spectral slopes of colored dissolved organic matter absorption with mixing and removal in a terrestrially dominated marine system (Hudson Bay, Canada), *Mar. Chem.*, *134*, 10–17, doi:10.1016/j.marchem.2012.02.008.

Granskog, M. A., R. W. Macdonald, C.-J. Mundy, and D. G. Barber (2007), Distribution, characteristics and potential impacts of chromophoric dissolved organic matter (CDOM) in Hudson Strait and Hudson Bay, Canada, *Cont. Shelf Res.*, *27*(15), 2032–2050, doi:10.1016/j.csr.2007.05.001.

Granskog, M. A., C. A. Stedmon, P. A. Dodd, R. M. W. Amon, A. K. Pavlov, L. de Steur, and E. Hansen (2012), Characteristics of colored dissolved organic matter (CDOM) in the Arctic outflow in the Fram Strait: Assessing the changes and fate of terrigenous CDOM in the Arctic Ocean, *J. Geophys. Res.*, *117*, C12021, doi:10.1029/2012JC008075.

Guéguen, C., and P. Kowalczuk (2013), Colored dissolved organic matter in frontal zones, in *Chemical Oceanography of Frontal Zones*, edited by I. M. Belkin, pp. 1–35, Springer-Verlag, Berlin Heidelberg, Berlin.

Ha, S. Y., Y. N. Kim, M. O. Park, S. H. Kang, H. C. Kim, and K. H. Shin (2012), Production of mycosporine-like amino acids of in situ phytoplankton community in Kongsfjorden, Svalbard, Arctic, *J. Photochem. Photobiol., B*, *114*, 1–14, doi:10.1016/j.jphotobiol.2012.03.011.

Helms, J. R., A. Stubbins, J. D. Ritchie, E. C. Minor, D. J. Kieber, and K. Mopper (2008), Absorption spectral slopes and slope ratios as indicators of molecular weight, source, and photobleaching of chromophoric dissolved organic matter, *Limnol. Oceanogr.*, *53*(3), 955–969.

Hill, V. J. (2008), Impacts of chromophoric dissolved organic material on surface ocean heating in the Chukchi Sea, *J. Geophys. Res.*, *113*, C07024, doi:10.1029/2007JC004119.

Intergovernmental Panel on Climate Change (2013), Summary for policymakers, in *Climate Change 2013: The Physical Science Basis. Contribution of Working Group I to the Fifth Assessment Report of the Intergovernmental Panel on Climate Change*, edited by, edited by T. F. Stocker et al., Cambridge Univ. Press, Cambridge, U. K. and New York.

Iversen, K. R., and L. Seuthe (2011), Seasonal microbial processes in a high-latitude fjord (Kongsfjorden, Svalbard): I. Heterotrophic bacteria, picoplankton and nanoflagellates, *Polar Biol.*, *34*(5), 731–749, doi:10.1007/s00300-010-0929-2.

©2014. American Geophysical Union. All Rights Reserved.

Johansen, B., and H. Tømmervik (2013), The relationship between phytomass, NDVI and vegetation communities on Svalbard, *Int. J. Appl. Earth Obs. Geoinf.*, *27*(A), 20–30, doi:10.1016/j.jag.2013.07.001.
Laxon, S. W., et al. (2013), CryoSat-2 estimates of Arctic sea ice thickness and volume, *Geophys. Res. Lett.*, *40*, 732–737, doi:10.1002/grl.50193.
Lehmann, M. K., R. F. Davis, Y. Huot, and J. J. Cullen (2004), Spectrally weighted transparency in models of water-column photosynthesis and its inhibition by ultraviolet radiation, *Mar. Ecol. Prog. Ser.*, *269*, 101–110, doi:10.3354/meps269101.
Lønborg, C., M. Middelboe, and C. P. Brussaard (2013), Viral lysis of Micromonas pusilla: impacts on dissolved organic matter production and composition, *Biogeochemistry*, *116*(1–3), 231–240, doi:10.1007/s10533-013-9853-1.
Manney, G. L., et al. (2011), Unprecedented Arctic ozone loss in 2011, *Nature*, *478*(7370), 469–475, doi:10.1038/nature10556.
Matsuoka, A., Y. Huot, K. Shimada, S. I. Saitoh, and M. Babin (2007), Bio-optical characteristics of the western Arctic Ocean: Implications for ocean color algorithms, *Can. J. Remote Sens.*, *33*, 503–518, doi:10.5589/m07-059.
Michalek-Wagner, K. (2001), Seasonal and sex-specific variations in levels of photo-protecting mycosporine-like amino acids (MAAs) in soft corals, *Mar. Biol.*, *139*(4), 651–660.
Nelson, N. B., and D. A. Siegel (2002), Chromophoric DOM in the open ocean, in *Biogeochemistry of Marine Dissolved Organic Matter*, edited by D. A. Hansell and C. A. Carlson, pp. 547–578, Academic Press, San Diego.
Nelson, N. B., D. A. Siegel, and A. F. Michaels (1998), Seasonal dynamics of colored dissolved material in the Sargasso Sea, *Deep Sea Res., Part I*, *45*(6), 931–957, doi:10.1016/S0967-0637(97)00106-4.
Nelson, N. B., C. A. Carlson, and D. K. Steinberg (2004), Production of chromophoric dissolved organic matter by Sargasso Sea microbes, *Mar. Chem.*, *89*(1), 273–287, doi:10.1016/j.marchem.2004.02.017.
Oren, A. (1997), Mycosporine-like amino acids as osmotic solutes in a community of halophilic cyanobacteria, *Geomicrobiol. J.*, *14*(3), 231–240.
Oren, A., and N. Gunde-Cimerman (2007), Mycosporines and mycosporine-like amino acids: UV protectants or multipurpose secondary metabolites?, *FEMS Microbiol. Lett.*, *269*(1), 1–10, doi:10.1111/j.1574-6968.2007.00650.x.
Osburn, C. L., L. Retamal, and W. F. Vincent (2009), Photoreactivity of chromophoric dissolved organic matter transported by the Mackenzie River to the Beaufort Sea, *Mar. Chem.*, *115*(1), 10–20, doi:10.1016/j.marchem.2009.05.003.
Pegau, W. S. (2002), Inherent optical properties of the central Arctic surface waters, *J. Geophys. Res.*, *107*(C10), 8035, doi:10.1029/2000JC000382.
Peterson, B. J., R. M. Holmes, J. W. McClelland, C. J. Vörösmarty, R. B. Lammers, A. I. Shiklomanov, I. A. Shiklomanov, and S. Rahmstorf (2002), Increasing river discharge to the Arctic Ocean, *Science*, *298*(5601), 2171–2173, doi:10.1126/science.1077445.
Polyakov, I. V., et al. (2005), One more step toward a warmer Arctic, *Geophys. Res. Lett.*, *32*, L17605, doi:10.1029/2005GL023740.
Polyakov, I. V., et al. (2011), Fate of early 2000s Arctic warm water pulse, *Bull. Am. Meteorol. Soc.*, *92*(5), 561–566, doi:10.1175/2010BAMS2921.1.
Pope, R. M., and E. S. Fry (1997), Absorption spectrum (380–700 nm) of pure water. II. Integrating cavity measurements, *Appl. Optics*, *36*(33), 8710–8723.
Popova, E. E., A. Yool, A. C. Coward, F. Dupont, C. Deal, S. Elliott, E. Hunke, M. Jin, M. Steele, and J. Zhang (2012), What controls primary production in the Arctic Ocean? Results from an intercomparison of five general circulation models with biogeochemistry, *J. Geophys. Res.*, *117*, C00D12, doi:10.1029/2011JC007112.
Post, E., U. S. Bhatt, C. M. Bitz, J. F. Brodie, T. L. Fulton, M. Hebblewhite, J. Kerby, S. J. Kutz, I. Stirling, and D. A. Walker (2013), Ecological consequences of sea-ice decline, *Science*, *341*(6145), 519–524, doi:10.1126/science.1235225.
Qian, J., and K. Mopper (1996), Automated high-performance, high-temperature combustion total organic carbon analyzer, *Anal. Chem.*, *68*(18), 3090–3097.
Řezanka, T., M. Temina, A. G. Tolstikov, and V. M. Dembitsky (2004), Natural microbial UV radiation filters—Mycosporine-like amino acids, *Folia Microbiol.*, *49*(4), 339–352.
Riebesell, U., J.-P. Gattuso, T. F. Thingstad, and J. J. Middelburg (2013a), Arctic ocean acidification: Pelagic ecosystem and biogeochemical responses during a mesocosm study, *Biogeosciences*, *10*, 5619–5626.
Riebesell, U., et al. (2013b), Technical note: A mobile sea-going mesocosm system—new opportunities for ocean change research, *Biogeosciences*, *10*, 1835–1847, doi:10.5194/bg-10-1835-2013.
Rochelle-Newall, E. J., and T. R. Fisher (2002), Production of chromophoric dissolved organic matter fluorescence in marine and estuarine environments: an investigation into the role of phytoplankton, *Mar. Chem.*, *77*(1), 7–21.
Rochelle-Newall, E. J., T. R. Fisher, C. Fan, and P. M. Glibert (1999), Dynamics of chromophoric dissolved organic matter and dissolved organic carbon in experimental mesocosms, *Int. J. Remote Sens.*, *20*(3), 627–641.
Rochelle-Newall, E., B. Delille, M. Frankignoulle, J. P. Gattuso, S. Jacquet, U. Riebesell, A. Terbrüggen, and I. Zondervan (2004), Chromophoric dissolved organic matter in experimental mesocosms maintained under different pCO2 levels, *Mar. Ecol. Progr. Ser.*, *272*, 25–31, doi:10.3354/meps272025.
Rochelle-Newall, E., F. D. Hulot, J. L. Janeau, and A. Merroune (2014), CDOM fluorescence as a proxy of DOC concentration in natural waters: A comparison of four contrasting tropical systems, *Environ. Monit. Assess.*, *186*(1), 589–596.
Romera-Castillo, C., H. Sarmento, X. A. Alvarez-Salgado, J. M. Gasol, and C. Marrasé (2010), Production of chromophoric dissolved organic matter by marine phytoplankton, *Limnol. Oceanogr.*, *55*(1), 446–454.
Schulz, K. G., et al. (2013), Temporal biomass dynamics of an Arctic plankton bloom in response to increasing levels of atmospheric carbon dioxide, *Biogeosciences*, *10*, 161–180, doi:10.5194/bg-10-161-2013.
Seuthe, L., K. R. Iversen, and F. Narcy (2011), Microbial processes in a high-latitude fjord (Kongsfjorden, Svalbard): II. Ciliates and dinoflagellates, *Polar Biol.*, *34*(5), 751–766, doi:10.1007/s00300-010-0930-9.
Siegel, D. A., S. Maritorena, N. B. Nelson, D. A. Hansell, and M. Lorenzi-Kayser (2002), Global distribution and dynamics of colored dissolved and detrital organic materials, *J. Geophys. Res.*, *107*(C12), 3228, doi:10.1029/2001JC000965.
Silyakova, A., R. G. J. Bellerby, K. G. Schulz, J. Czerny, T. Tanaka, G. Nondal, U. Riebesell, A. Engel, T. De Lange, and A. Ludvig (2013), Pelagic community production and carbon-nutrient stoichiometry under variable ocean acidification in an Arctic fjord, *Biogeosciences*, *10*, 4847–4859, doi:10.5194/bg-10-4847-2013.
Spencer, R. G., G. R. Aiken, K. D. Butler, M. M. Dornblaser, R. G. Striegl, and P. J. Hernes (2009), Utilizing chromophoric dissolved organic matter measurements to derive export and reactivity of dissolved organic carbon exported to the Arctic Ocean: A case study of the Yukon River, Alaska, *Geophys. Res. Lett.*, *36*, L06401, doi:10.1029/2008GL036831.
Stedmon, C. A., and S. Markager (2001), The optics of chromophoric dissolved organic matter (CDOM) in the Greenland Sea: An algorithm for differentiation between marine and terrestrially derived organic matter, *Limnol. Oceanogr.*, *46*(8), 2087–2093, doi:10.4319/lo.2001.46.8.2087.

©2014. American Geophysical Union. All Rights Reserved.

Stedmon, C. A., R. M. W. Amon, A. J. Rinehart, and S. A. Walker (2011), The supply and characteristics of colored dissolved organic matter (CDOM) in the Arctic Ocean: Pan Arctic trends and differences, *Mar. Chem.*, *124*(1), 108–118, doi:10.1016/j.marchem.2010.12.007.

Steinberg, D. K., N. B. Nelson, C. A. Carlson, and A. C. Prusak (2004), Production of chromophoric dissolved organic matter (CDOM) in the open ocean by zooplankton and the colonial cyanobacterium Trichodesmium spp, *Mar. Ecol. Progr. Ser.*, *267*(1), 45–56.

Stroeve, J. C., V. Kattsov, A. Barrett, M. Serreze, T. Pavlova, M. Holland, and W. N. Meier (2012), Trends in Arctic sea ice extent from CMIP5, CMIP3 and observations, *Geophys. Res. Lett.*, *39*, L16502, doi:10.1029/2012GL052676.

Svalbard 2010 team (2010), EPOCA Svalbard 2010 mesocosm experiment in Kongsfjorden, Svalbard, Norway, doi:10.1594/PANGAEA.769833.

Svendsen, H., et al. (2002), The physical environment of Kongsfjorden-Krossfjorden, an Arctic fjord system in Svalbard, *Polar Res.*, *21*(1), 133–166, doi:10.1111/j.1751-8369.2002.tb00072.x.

Uusikivi, J., A. V. Vähätalo, M. A. Granskog, and R. Sommaruga (2010), Contribution of mycosporine-like amino acids and colored dissolved and particulate matter to sea ice optical properties and ultraviolet attenuation, *Limnol. Oceanogr.*, *55*(2), 703–713.

Vernet, M., and K. Whitehead (1996), Release of ultraviolet-absorbing compounds by the red-tide dinoflagellate Lingulodinium polyedra, *Mar. Biol.*, *127*(1), 35–44, doi:10.1007/BF00993641.

Vonk, J. E., et al. (2012), Activation of old carbon by erosion of coastal and subsea permafrost in Arctic Siberia, *Nature*, *489*(7414), 137–140, doi:10.1038/nature11392.

Walczowski, W., and J. Piechura (2007), Pathways of the Greenland Sea warming, *Geophys. Res. Lett.*, *34*, L10608, doi:10.1029/2007GL029974.

Whitehead, K., and M. Vernet (2000), Influence of mycosporine-like amino acids (MAAs) on UV absorption by particulate and dissolved organic matter in La Jolla Bay, *Limnol. Oceanogr.*, *45*(8), 1788–1796.

Zhang, Y., Y. Yin, X. Liu, Z. Shi, L. Feng, M. Liu, G. Zhua, Z. Gonga, and B. Qin (2011), Spatial-seasonal dynamics of chromophoric dissolved organic matter in Lake Taihu, a large eutrophic, shallow lake in China, *Org. Geochem.*, *42*(5), 510–519, doi:10.1016/j.orggeochem.2011.03.007.

©2014. American Geophysical Union. All Rights Reserved.